using the action of the normalizer of the point group. Two point groups, arithmetically equivalent as n-dimensional point groups, can be arithmetically nonequivalent when considered as describing quasi-periodic structures. This gives a further partition of the arithmetic crystal classes.

References

ASCHER, E. & JANNER, A. (1965). *Helv. Phys. Acta*, **38**, 551-572.
BAAKE, M., JOSEPH, D. & SCHLOTTMANN, M. (1991). *Int. J. Mod. Phys.* B**5**, 1927-1953.
BAK, P. (1985). *Phys. Rev. B*, **32**, 5764-5772.
BOHR, H. (1924). *Acta Math.* **45**, 29-127.
BROWN, H., BÜLOW, R., NEUBÜSER, J., WONDRATSCHEK, H. & ZASSENHAUS, H. (1978). *The Crystallographic Groups of Four-Dimensional Space.* New York: Wiley.
BÜLOW, R. (1973). Dissertation, RWTH, Aachen, Germany.
FAST, G. & JANSSEN, T. (1971). *J. Comput. Phys.* **7**, 1-11.
FROBENIUS, G. & SCHUR, I. (1906). *Sitzungsber. K. Preuss. Akad. Wiss.* 186-208.
International Tables for Crystallography (1989). Vol. A. Dordrecht: Kluwer Academic Publishers.
JANNER, A. & JANSSEN, T. (1979). *Physica (Utrecht)*, A**99**, 47-76.
JANNER, A. & JANSSEN, T. (1980*a*). *Acta Cryst.* A**36**, 399-408.
JANNER, A. & JANSSEN, T. (1980*b*). *Acta Cryst.* A**36**, 408-415.
JANNER, A., JANSSEN, T. & DE WOLFF, P. M. (1983). *Acta Cryst.* A**39**, 658-666.
JANSEN, L. & BOON, M. (1967). *Theory of Finite Groups. Applications in Physics.* Amsterdam: North-Holland.
JANSSEN, T. (1986). *Acta Cryst.* A**42**, 261-271.
JANSSEN, T. (1988). *Phys. Rep.* **168**, 55-113.
JANSSEN, T. (1990). In *Quasicrystals.* Springer Series in Solid-State Sciences 93, edited by T. FUJIWARA & T. OGAWA. Berlin: Springer.
JANSSEN, T. (1991). *Acta Cryst.* A**47**, 243-255.
JANSSEN, T. (1992). *Z. Kristallogr.* **198**, 17-32.
JANSSEN, T. & JANNER, A. (1987). *Adv. Phys.* **36**, 519-624.
JANSSEN, T., JANNER, A. & ASCHER, E. (1969). *Physica (Utrecht)*, **42**, 41-70.
KRAMER, P. (1987). *Acta Cryst.* A**43**, 486-489.
PLESKEN, W. & POHST, M. (1977). *Math. Comput.* **31**, 536-551, 552-573.
PLESKEN, W. & POHST, M. (1980). *Math. Comput.* **34**, 245-258, 259-275, 277-301.
RYSKOV, S. (1972*a*). *Dokl. Akad. Nauk SSSR*, **204**, 561-564; Engl. transl: *Sov. Math. Dokl.* **13**, 720-724.
RYSKOV, S. (1972*b*). *Tr. Mat. Inst. Steklov.* **128**, 183-211; Engl. transl: *Proc. Steklov. Inst. Math.* **128**, 217-250.
WIJNANDS, F. (1991). *J. Phys. A*, **24**, 5703-5720.
WIJNANDS, F. & THIERS, A. (1992). *J. Math. Phys.* **33**, 1601-1611.
WOLFF, P. M. DE (1974). *Acta Cryst.* A**30**, 777-785.
WOLFF, P. M. DE, JANSSEN, T. & JANNER, A. (1981). *Acta Cryst.* A**37**, 625-636.
YAMAMOTO, A. (1982). *Acta Cryst.* B**38**, 1451-1456.

Acta Cryst. (1993). A**49**, 324-330

On the Sign Ambiguity of Triplet Phases in Nonsystematic Many-Beam Effects in CBED Patterns

BY K. MARTHINSEN

SINTEF Applied Physics, N-7034 Trondheim, Norway

(*Received* 18 *June* 1992; *accepted* 20 *August* 1992)

Abstract

The possibility to determine not only the magnitude but also the sign of three-phase structure invariants from nonsystematic many-beam effects in convergent-beam electron diffraction (CBED) patterns is discussed. From the full dynamical many-beam intensity expression it is clear that it is a principal difference between equivalent three-beam cases of opposite sign of the triplet phases. However, the difference and thus the ability to distinguish between the two cases depends strongly both on the relative magnitude of the structure factors involved and the specimen thickness for which the actual CBED discs are obtained. The largest differences are obtained for a weakly coupled three-beam case where the intensity in the line of the primary reflection, which in this case coincides with the kinematical two-beam position, has a distinct maximum or minimum at the three-beam condition depending on the sign of the triplet phase. In a strong coupling case where the intensity in the primary-reflection line near the three-beam condition is split into two individual segments, the differences are generally less and are not so obvious and quantitative measurements are necessary to distinguish the two cases of opposite sign of the triplet phases. Calculated examples with respect to a nonsystematic three-beam example in the noncentrosymmetric InP are given.

Introduction

A general convergent-beam electron diffraction (CBED) method for quantitative determination of structure-factor magnitudes and phases from centrosymmetric as well as noncentrosymmetric crystals

0108-7673/93/020324-07$06.00

has recently been suggested (Høier, Zuo, Marthinsen & Spence, 1988; Marthinsen, Runde, Holmestad & Høier, 1991). It is based on detailed simulations of nonsystematic many-beam diffraction effects, which by least-square techniques and iterative calculations are fitted to the observed two-dimensional distributions in the discs. The basis for the phase determination is intensity asymmetries, which may appear in a line **g** with respect to the Bragg condition of strongly coupled reflections **h** near a many-beam condition. For qualitative purposes, these intensity variations may in most cases be interpreted in terms of three-beam interactions and by means of approximative analytical three-beam expressions such as, for instance, the second Bethe approximation (Zuo, Høier & Spence, 1989), or Kambe's strong-coupling approximation (Kambe, 1957). These expressions indicate the basis for the suggested structure-factor-refinement method and that the complicated two-dimensional intensity variations in favorable cases may depend strongly on both the structure-factor magnitudes $|U_g|$ and the phases φ_g of the reflections **h** involved. As for the phase dependence, it enters the approximative expressions through a term $\cos\psi$, where ψ is the so-called three-phase structure invariant, *i.e.* $\psi=\varphi_{-g}+\varphi_h+\varphi_{g-h}$. Owing to the cosine term, this means that, in principle, only the absolute value of the phase invariant can be determined, while the sign is apparently not available.

However, as will be shown below, this apparent sign ambiguity is a result of the approximations made. Examining the full dynamical many-beam intensity expression shows that differences should be expected for many-beam cases of opposite triplet phases. The aim of the present work is to discuss the origin of these differences and the general possibility of distinguishing $\pm\psi$ for different many-beam interactions (arbitrary reflections and couplings) and for different thicknesses. In the present work, we discuss these aspects by means of calculated many-beam examples from the noncentrosymmetric InP. Some preliminary results of this work have already been presented (Marthinsen & Høier, 1989).

Theory

The Bloch-wave formulation of dynamical electron diffraction theory is based on a Fourier expansion of the periodic potential $U(\mathbf{r})$ in the reciprocal-lattice vectors **g** (Bethe, 1928; Humphreys, 1979), *i.e.*

$$U(\mathbf{r})=\sum_{\mathbf{g}} U_{\mathbf{g}}\exp(i\mathbf{g}\cdot\mathbf{r}), \tag{1}$$

and the wave function of the electrons propagating through the crystal on Bloch form

$$\psi(\mathbf{r})=\sum_{\mathbf{g}} C_{\mathbf{g}}\exp[i(\mathbf{k}+\mathbf{g})\cdot\mathbf{r}]. \tag{2}$$

Inserting (1) and (2) into the time-independent Schrödinger equation gives the so-called fundamental equation of high-energy electron diffraction, *viz*

$$[K^2-(\mathbf{k}^i+\mathbf{g})^2]C^i_{\mathbf{g}}+\sum_{\mathbf{h}\neq\mathbf{g}} U_{\mathbf{g}-\mathbf{h}}C^i_{\mathbf{h}}=0, \tag{3}$$

there being one such equation i for each reflection **g** considered. Here $K^2=\chi^2+U_0$, where χ is the wave vector of the incident electron wave in vacuum and U_0 is the mean inner crystal potential. The electron structure factor $U_g=8\pi^2 meV_g/h^2$, where V_g is a Fourier coefficient of the crystal potential $V(\mathbf{r})$ in V and m is the relativistically corrected electron mass. In the case of a noncentrosymmetric crystal where $U(\mathbf{r})\neq U(-\mathbf{r})$, U_g will in general be a complex quantity with both an amplitude and a phase, *i.e.*

$$U_g=|U_g|\exp(i\varphi_g). \tag{4}$$

Equation (3) may be rewritten in a more convenient form by introducing the *Anpassungen* γ^i and the excitation error s_g. The *Anpassungen* γ^i are the fine adjustments at the entrance surfaces of the mean crystal wave vectors that are necessary to obtain dynamical equilibrium for the interacting Bloch waves in the crystal; they are defined by

$$\mathbf{k}^i=\mathbf{K}-\gamma^i\mathbf{n}. \tag{5}$$

Here **n** is a unit vector along the normal of the crystal entrance surface. The excitation error s_g is the distance from the reciprocal-lattice point **g** to the Ewald sphere (defined positive inside the sphere), *i.e.*

$$2Ks_g=K^2-(\mathbf{K}+\mathbf{g})^2. \tag{6}$$

Considering only reflections of the zero-order Laue zone (ZOLZ), inserting (5) and (6) into (3) and neglecting higher-order terms in the small quantities s_g and γ^i, we obtain the set of eigenvalue equations

$$2Ks_gC^i_{\mathbf{g}}+\sum_{\mathbf{h}\neq\mathbf{g}} U_{\mathbf{g}-\mathbf{h}}C^i_{\mathbf{h}}=2K\gamma^iC^i_{\mathbf{g}}. \tag{7}$$

With n beams involved there are n such equations that may be solved to give n Bloch-wave eigenvalues γ^i and n Bloch-wave eigenvectors with n elements $C^i_{\mathbf{g}}$. These elements will in the general case of a noncentrosymmetric crystal be complex quantities, although the eigenvalues (without absorption) are real. The electron wave function for the diffracted beam **g** is then given by

$$\psi_{\mathbf{g}}(\mathbf{r})=\sum_i C^{i*}_0C^i_{\mathbf{g}}\exp[i(\mathbf{k}^i+\mathbf{g})\cdot\mathbf{r}], \tag{8}$$

where C^{i*}_0 is introduced to take care of the boundary conditions at the entrance surface. The intensity at the exit surface of a crystal slab of thickness t of a particular Bragg beam **g** is then (with absorption neglected) found from

$$I_{\mathbf{g}}(t)=\sum_i\sum_j C^{i*}_0C^i_{\mathbf{g}}C^j_0C^{j*}_{\mathbf{g}}\exp[i(\gamma^i-\gamma^j)t]. \tag{9}$$

If we explicitly take into account the fact that the

eigenvector components are complex quantities, (9) may be written as

$$I_{\mathbf{g}}(t) = \sum_i |C_0^{i*} C_{\mathbf{h}}^i|^2 + 2 \sum_{i>j} |C_0^{i*} C_{\mathbf{g}}^i C_0^j C_{\mathbf{g}}^{j*}| \cos[(\gamma^i - \gamma^j)t + \Omega_{ij}], \quad (10)$$

where Ω_{ij} is the phase of $C_0^{i*} C_{\mathbf{g}}^i C_0^j C_{\mathbf{g}}^{j*}$.

The understanding of the differences between cases with triplet phases of opposite sign, *i.e.* $\pm\psi$, is provided by (10). The origin of the intensity differences lies in the phase Ω_{ij}. To understand this point, consider the two enantiomorphic forms of a noncentrosymmetric space group: the structure (S) with atomic coordinates r_j and the inverse (I) with atomic coordinates $r_j' = -r_j$. With the same choice of origin for both forms, the structure factors $U_{\mathbf{g}}$ will have the same amplitudes but phases of opposite signs, $\pm\varphi$. Consequently, the triplet phases will also have opposite signs. Solving a particular many-beam case for these two cases will then give the same eigenvalues but complex-conjugate eigenvector sets. With reference to (10), this implies that the two cases will have the same magnitude but opposite signs of the phases Ω_{ij}. This sign difference gives generally different intensities for the two cases. However, the magnitude of this difference is expected to depend strongly on both the diffraction condition and the thickness at which the experiment takes place.

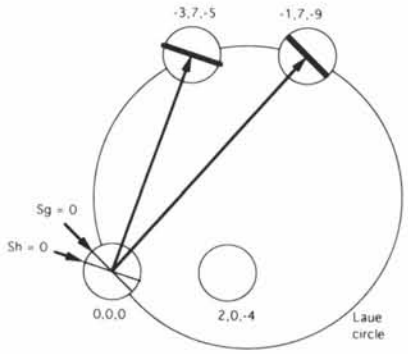

Fig. 1. The 000, −3,7,−9, −1,7,−9 three-beam case used in the calculated examples. Arrows show the simultaneous Bragg condition.

Calculated three-beam examples

To illustrate and discuss the possibilities of distinguishing triplet phases of $\pm\psi$ in CBED patterns, we have considered a particular three-beam example from InP, *viz* the 000, $\mathbf{h} = -3,7,-5$, $\mathbf{g} = -1,7,-9$ case and the intensity variations in the −1,7,−9 disc. A diagram of this diffraction case is shown in Fig. 1. To calculate the CBED disc intensities we have used the CBED-simulation program of Zuo, Gjønnes & Spence (1989). Calculations have been performed at an accelerating voltage of 250 kV and at thicknesses of 1100 and 2200 Å. To determine the effect of changing the sign of the invariant-phase sum and how this affects the CBED disc intensities for different couplings between the reflections involved, the structure-factor amplitudes and phases were changed in calculations to obtain the desired phase sums and amplitude ratios. This investigation was particularly focused on cases with phase triplets of $\psi = \pm\pi/2$. In these cases there are, according to the second Bethe approximation and the Kambe approximation, no asymmetries in the intensities since the $\cos\psi$ term for these particular values of ψ disappears.

In the first calculated example we have used theoretically correct atomic structure-factor amplitudes, while the structure-factor phases, however, are artificially chosen to give phase sums of $+\pi/2$ and $-\pi/2$, respectively. This is a so-called weak-coupling case with the amplitude ratio $\alpha =$

(*a*) (*b*) (*c*)

Fig. 2. Calculated CBED disc intensity in the −1,7,−9 disc. $|U_{-3,7,-5}||U_{2,0,-4}|/|U_{-1,7,-9}| = 0.028$, $t = 1100$ Å, $E = 250$ keV. (*a*) $\psi = \pi/2$; (*b*) $\psi = -\pi/2$; (*c*) intensity difference between patterns in (*a*) and (*b*); $\Delta I/I = 0.98$. Note that the intensity in each pattern is scaled to its own maximum.

$|U_{-3,7,-5}||U_{2,0,-4}|/|U_{-1,7,-9}| = 0.028$. The calculated intensities in the $\mathbf{g} = -1,7,-9$ disc for the two cases at 1100 Å are shown in Figs. 2(*a*) and (*b*). We notice clear differences between the two cases that should be easily observable: the $\pi/2$ case has a large intensity maximum at the kinematical three-beam condition and the $-\pi/2$ case has a clear minimum. The difference is illustrated explicitly in Fig. 2(*c*), which shows the intensity difference between the patterns in Figs. 2(*a*) and (*b*). Note that the intensity in each of the three patterns in Fig. 2 is scaled to its own maximum. This is also the case for all the other patterns of this type presented here. As a quantitative measure of the difference, the quantity

$$\Delta I/I = \max |I^i_{\psi=\pi/2} - I^i_{\psi=-\pi/2}|/I^i_{\psi=\pi/2} \qquad (11)$$

has been used, where I^i refers to the intensity of pixel *i*. For the pattern in Fig. 2(*c*), $\Delta I/I = 0.98$. This large difference is also seen in Fig. 3, where the intensity along the ridge of the $\mathbf{g} = -1,7,-9$ line through the three-beam condition is shown. In this case, the structure-factor amplitudes and their ratios are such that the position of maximum intensity coincides with the kinematical two-beam position ($s_g = 0$) for the $-1,7,-9$ line except very near the three-beam condition for the $\psi = -\pi/2$ case. The result of going along the kinematical-line position in this region is illustrated by the lower curve in Fig. 3. This is a so-called weak-coupling case and the results are in agreement with the results of Bird, James & Preston (1987) using a kinematic weak-beam approximation to model three-beam phase effects in CBED.

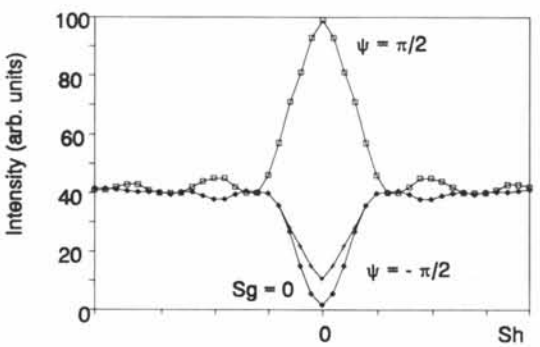

Fig. 3. Intensity variation along the ridge of the $-1,7,-9$ line in Figs. 2(*a*) and (*b*).

However, the magnitude of the differences is highly dependent on the specimen thickness. Figs. 4(*a*) and (*b*) show the same diffraction cases as in Figs. 2(*a*) and (*b*) but at 2200 Å. One sees immediately that the differences are not so pronounced as in Fig. 2 ($\Delta I/I = 0.43$). The differences, shown in Fig. 4(*c*), are both less pronounced and more localized than in Fig. 2(*c*). The intensity variations along the kinematical-line position for the two cases are shown in Fig. 5. It is clearly seen that the relative differences are much less than in Fig. 3 and the differences are less obvious due to the rapid intensity oscillations near the three-beam position. This means that for this particular example it is more difficult to distinguish the two cases of opposite signs of the triplet phases at a thickness of 2200 than at 1100 Å.

In the second example, the structure-factor amplitude for the coupling reflection, *i.e.* $U_{2,0,-4}$, is artificially increased by a factor of 8. The phases, however, are kept unchanged. The amplitude ratio α is now 0.22, and in this case, which is a strong-coupling case, the $-1,7,-9$ line splits into two segments with a width between the two segments proportional to $U_{2,0,-4}$ (Gjønnes & Høier, 1971). The resulting CBED disc intensities at 1100 Å are shown in Figs. 6(*a*) and (*b*). It is difficult to observe any qualitative differences, although the quantitative differences, as seen from Fig. 6(*c*), are quite clear. The relative differences ($\Delta I/I$) are about 20–25% at maximum and are limited to the regions of maximum intensity, *i.e.* along the split-intensity hyperbolas. However, with good quantitative intensity data it should be fairly easy to distinguish the two cases of

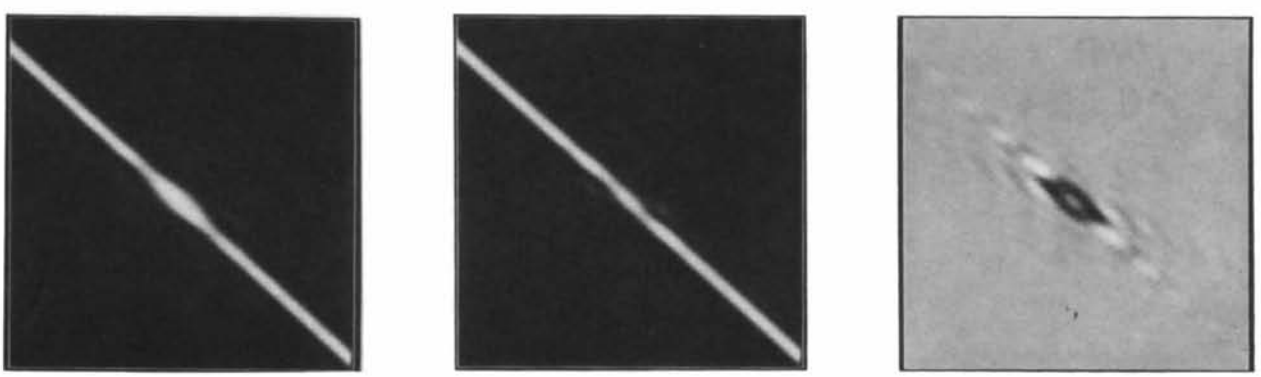

(*a*) (*b*) (*c*)

Fig. 4. Calculated CBED disc intensity in the $-1,7,-9$ disc. $|U_{-3,7,-5}||U_{2,0,-4}|/|U_{-1,7,-9}| = 0.028$, $t = 2200$ Å, $E = 250$ keV. (*a*) $\psi = \pi/2$; (*b*) $\psi = -\pi/2$; (*c*) intensity difference between patterns in (*a*) and (*b*); $\Delta I/I = 0.43$. Intensity in each pattern scaled to its own maximum.

opposite sign of the phase triplet. Taking the intensity profiles along the kinematical line position of the $-1,7,-9$ line in this case gives practically no difference.

The corresponding intensity variations at 2200 Å for this example with $\alpha = 0.22$ are shown in Fig. 7. As in the first example, the differences are less at this thickness than at 1100 Å. In this case, the differences are only about 10% at maximum. So although there is a difference, and it is in principle possible to distinguish the two cases, it may be very difficult to carry out in practice. It will require very good experiments and accurate and reliable quantitative intensity data.

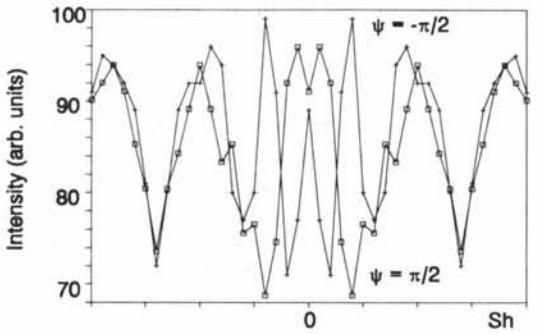

Fig. 5. Intensity variation along the ridge of the $-1,7,-9$ line in Figs. 4(a) and (b).

Finally, we carried out the same calculations for the present three-beam diffraction case using the correct structure-factor amplitudes and phases and the same case with opposite signs of the phases. The triplet phases are then either +39.2 or −39.2°. The calculated CBED disc intensities at 1100 and 2200 Å are shown in Fig. 8 together with the corresponding difference maps. In both cases, the differences are reasonably large, although not so obvious from a qualitative visual inspection alone. The relative differences are approximately three times as large at 1100 as at 2200 Å ($\Delta I/I = 0.65$ and 0.20, respectively). At 2200 Å the differences are also localized to a more limited region than at 1100 Å and for that reason it may be more difficult to distinguish the two cases of $\pm\psi$.

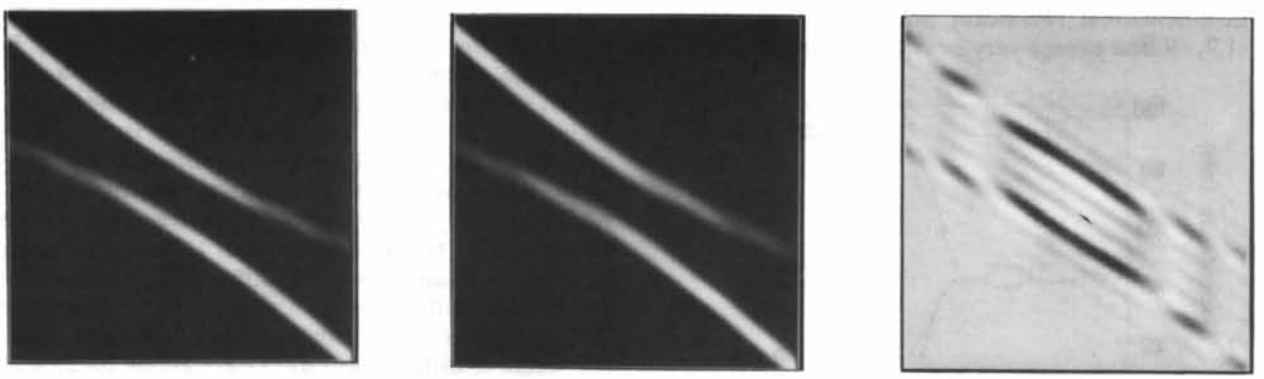

(a) (b) (c)

Fig. 6. Calculated CBED disc intensity in the $-1,7,-9$ disc. $|U_{-3,7,-5}||U_{2,0,-4}|/|U_{-1,7,-9}| = 0.22$, $t = 1100$ Å, $E = 250$ keV. (a) $\psi = \pi/2$; (b) $\psi = -\pi/2$; (c) intensity difference between patterns in (a) and (b); $\Delta I/I = 0.23$. Intensity in each pattern scaled to its own maximum.

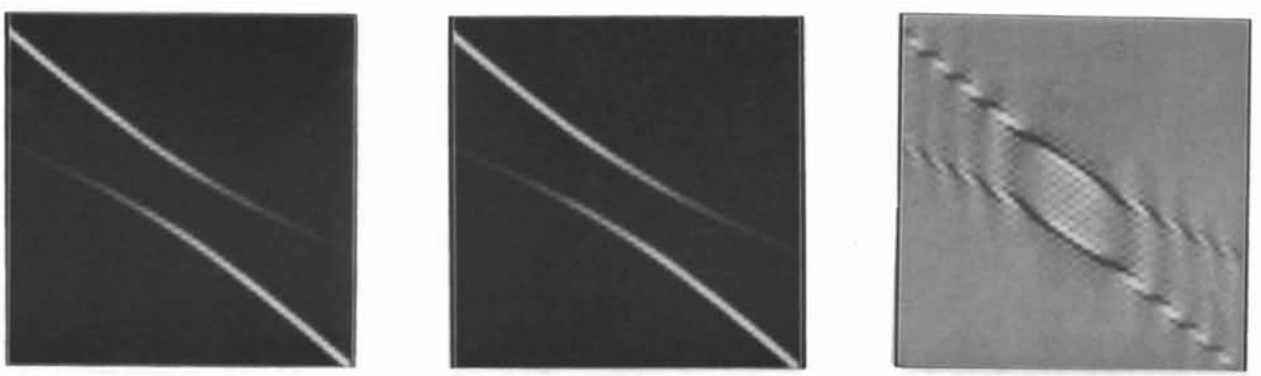

(a) (b) (c)

Fig. 7. Calculated CBED disc intensity in the $-1,7,-9$ disc. $|U_{-3,7,-5}||U_{2,0,-4}|/|U_{-1,7,-9}| = 0.22$, $t = 2200$ Å, $E = 250$ keV. (a) $\psi = \pi/2$; (b) $\psi = -\pi/2$; (c) intensity difference between patterns in (a) and (b); $\Delta I/I = 0.1$. Intensity in each pattern scaled to its own maximum.

Discussion and concluding remarks

We have in the present work discussed the possibility of determining not only the magnitude but also the sign of three-phase structure invariants from nonsystematic many-beam effects in CBED patterns. It is demonstrated that this sign information, in principle, is always present; however, the ease with which this sign information may be retrieved from experiments depends strongly on the magnitude of the individual structure factors involved and on the thickness at which the CBED patterns are obtained. The difference that may be observed between three-beam cases of opposite signs for their triplet phases is in general only accounted for by the full dynamical many-beam intensity expression. However, in the special case of small thicknesses and/or weak couplings, the kinematical weak-beam approximation of Bird, James & Preston (1987) is fully adequate. The second Bethe approximation and Kambe's weak-beam approximation, however, cannot account for the effect of sign difference. Both these approximative analytical approaches are based on approximations that eliminate the intensity differences caused by a sign shift in the triplet phase.

It should be mentioned in this connection that the phase factor Ω_{ij} in (10) is also the origin of the differences in the $\pm\mathbf{g}$ CBED disc intensities from a noncentrosymmetric crystal, which is actually the basis for determination of noncentrosymmetry with the CBED method (Buxton, Eades, Steeds & Rackham, 1976; Marthinsen, 1991). Since this phase factor appears in the thickness-dependent inter-Bloch-wave terms it also explains why observation of noncentrosymmetry or determination of enantiomorphs is in general difficult from Kikuchi patterns and electron channeling patterns (ECP), where these terms are expected to be integrated out. However, this is not always the case, as deviations from centrosymmetry have also been observed from electron channelling patterns (Marthinsen & Høier, 1988).

For a given thickness, the most pronounced differences between cases of opposite sign of the triplet phases will be found where the thickness-dependent terms in (10) are largest. In general, this is along the positions of maximum intensity. In a

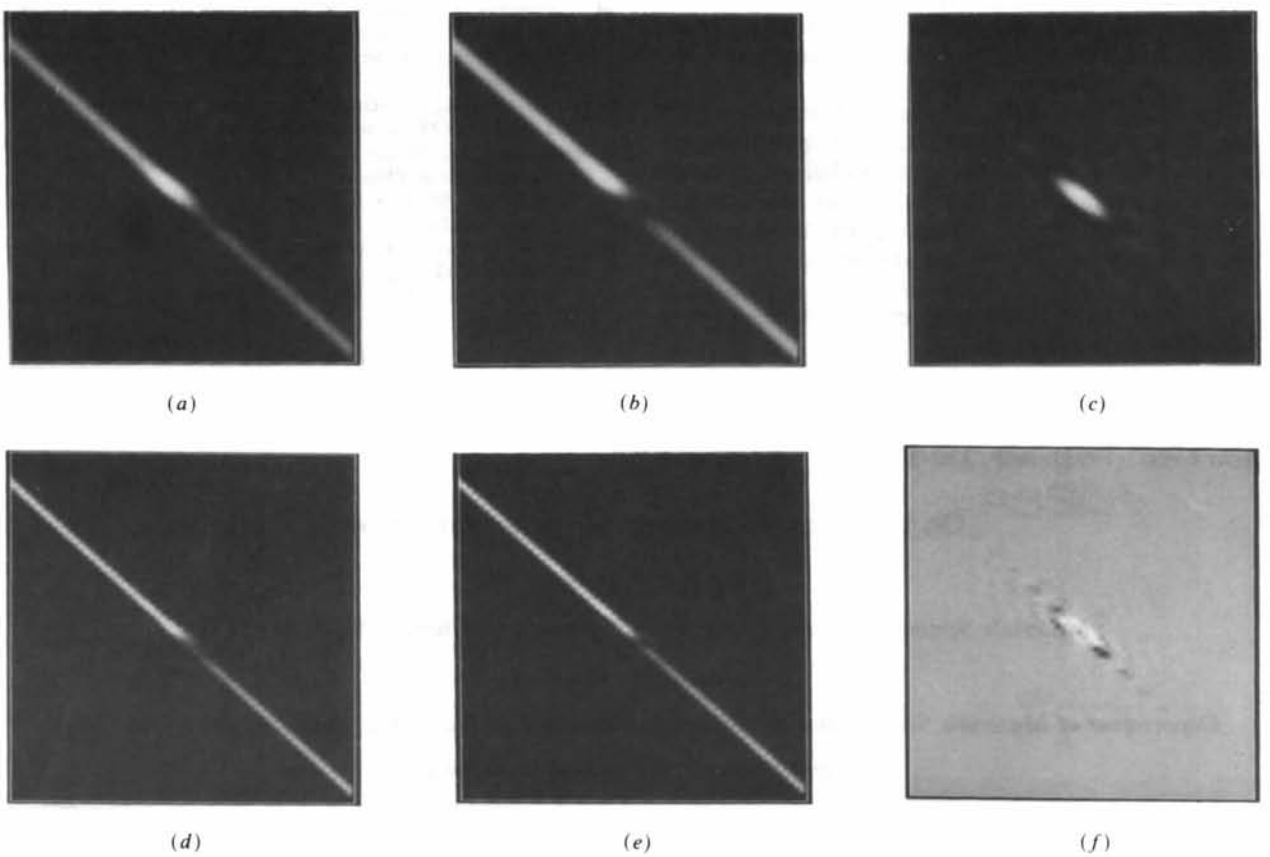

Fig. 8. Calculated CBED disc intensity in the $-1,7,-9$ disc. $|U_{-3,7,-5}||U_{2,0,-4}|/|U_{-1,7,-9}| = 0.028$, $E = 250$ keV. (*a*) $\psi = 39.2°$, $t = 1100$ Å; (*b*) $\psi = -39.2°$, $t = 1100$ Å; (*c*) intensity difference between patterns in (*a*) and (*b*); $\Delta I/I = 0.65$. (*d*) $\psi = 39.2°$, $t = 2200$ Å; (*e*) $\psi = -39.2°$, $t = 2200$ Å; (*f*) intensity difference between patterns in (*d*) and (*e*); $\Delta I/I = 0.2$. Intensity in each pattern scaled to its own maximum.

weak-coupling case this coincides more or less with the kinematical line position of the line in question, however in the case of strong coupling, a line **g** will split into two branches and each of these may be considerably displaced from the kinematical two-beam position near the three- (many-) beam condition (Høier, Zuo, Marthinsen & Spence, 1988). The largest differences between cases of opposite signs of the triplet phase seems to be for the former case where the two cases have a clear maximum or minimum near the kinematical three-beam condition. However, in the strong-coupling case relatively large quantitative differences may also be observed but the magnitude of the differences and thus the possibility to distinguish cases of opposite triplet phases is strongly dependent on the thickness.

However, it is difficult to find any simple rule as to which thicknesses give the largest differences. This is because the intensity difference in general is the result of the difference between several thickness-dependent terms in the intensity expression [(10)], each depending on the magnitude of a product of eigenvector components and a cosine term for which the argument is a sum of a t-dependent term and the phase of the product of eigenvector components in the prefactor. It is impossible to draw any general conclusions about which thicknesses maximize this complicated difference term.

In general, the determination of the correct sign of a triplet phase has to be based on high-quality experiments and quantitative intensity recordings. To avoid thickness averaging, which may blur the intensity variations of interest, CBED patterns should be obtained from parallel-sided specimens or the area from which the patterns are obtained should be so small that possible thickness variations are negligible. Experiments should further be carried out at liquid-nitrogen temperature using a cooling holder to minimize thermal diffuse scattering. Finally, quantitative comparisons should preferentially be based on digitized energy-filtered intensity data. Instrumentation for acquiring intensity data in this latter way are now under development and the use of such systems will increase the potential for quantitative CBED considerably in the future (see, for example, Spence, Mayer & Zuo, 1991; Marthinsen, Runde, Holmestad & Høier, 1991).

References

BETHE, H. (1928). *Ann. Phys. (Leipzig)*, **87**, 55-129.

BIRD, D. M., JAMES, R. & PRESTON, A. R. (1987). *Phys. Rev. Lett.* **59**, 1216-1219.

BUXTON, B. F., EADES, J. A., STEEDS, J. W. & RACKHAM, G. M. (1976). *Philos. Trans. R. Soc. London Ser. A*, **281**, 171-194.

GJØNNES, J. & HØIER, R. (1971). *Acta Cryst.* A**27**, 313-316.

HØIER, R., ZUO, J. M., MARTHINSEN, K. & SPENCE, J. C. H. (1988). *Ultramicroscopy*, **26**, 25-30.

HUMPHREYS, C. J. (1979). *Rep. Prog. Phys.* **42**, 1825-1887.

KAMBE, K. (1957). *J. Phys. Soc. Jpn*, **12**, 1-13.

MARTHINSEN, K. (1991). Report STF19 A91039. SINTEF, Trondheim, Norway.

MARTHINSEN, K. & HØIER, R. (1988). *Acta Cryst.* A**44**, 558-562.

MARTHINSEN, K. & HØIER, R. (1989). *Proc. 47th Annu. Meet. Electron Microsc. Soc. Am.*, edited by G. W. BAILY, pp. 484-485. San Francisco Press.

MARTHINSEN, K., RUNDE, P., HOLMESTAD, R. & HØIER, R. (1991). *Electron Microscopy and Analysis* 1991. *Inst. Phys. Conf. Series* No. 119, edited by F. J. HUMPHREYS, pp. 367-370. Bristol: Institute of Physics.

SPENCE, J. C. H., MAYER, J. & ZUO, J. M. (1991). *Micron Microsc. Acta*, **22**, 173-174.

ZUO, J. M., GJØNNES, K. & SPENCE, J. C. H. (1989). *J. Electron Microsc. Tech.* **12**, 29-55.

ZUO, J. M., HØIER, R. & SPENCE, J. C. H. (1989). *Acta Cryst.* A**45**, 839-851.

Acta Cryst. (1993). A**49**, 330-335

On the X-ray Reflectivity of Absorbing Crystals

BY P. D. MORAN

Materials Science Program, University of Wisconsin, Madison, WI 53706, *USA*

AND R. J. MATYI

Department of Materials Science and Engineering, University of Wisconsin, Madison, WI 53706, *USA*

(*Received* 28 *January* 1992; *accepted* 21 *August* 1992)

Abstract

A simple relationship is reported defining the ratio of dynamical and kinematic values of the integrated reflectivity in absorbing single crystals in terms of the product $\mu_n\xi$, where μ_n is the linear absorption coefficient for depth measured along the normal to the diffracting crystal's surface and ξ is the extinction distance in a nonabsorbing crystal. This relationship is interpreted through comparison with existing

0108-7673/93/020330-06$06.00